

Experimental Studies on the Kinetic Behavior of Water Boiler Type Reactors

By M. E. Remley, J. W. Flora, D. L. Hetrick, D. R. Muller, E. L. Gardner
R. E. Wimmer, R. K. Stitt and D. P. Gamble*

Early experimental investigations of the dynamic behavior of water boiler type reactors were conducted on the SUPO reactor at Los Alamos by Kasten,¹ and on the Livermore reactor by Flora, Shortall, and Drummond.² These experiments included reactivity releases up to a maximum of only about 0.4%, resulting in minimum reactor periods of about six seconds.

The present efforts on Kinetic Experiments on Water Boilers, known as the KEWB Program, were initiated as a full scale experimental study of the dynamic behavior of homogeneous solution reactors.³ The program objectives are aimed at extending the knowledge and understanding of the dominant parameters in the dynamic behavior and the safety of these types of reactors. The operating parameters which bear directly on the transient behavior of the reactor and are planned for investigation include the amount of reactivity released, the initial fuel temperature, the initial core pressure, and the initial power level.

The approach in the program has been to construct a prototype reactor with the special provisions required for the experimental transient studies. This prototype reactor is installed in a special test facility, which includes an underground building to house the reactor test cores with reflector, gas handling system and associated equipment, a waste disposal system, a small building containing amplifiers and power supplies, and the control building, some 200 ft from the test building.

The test reactor, a perspective view of which is shown in Fig. 1, is designed for a nominal power rating of 50 kilowatts. The stainless steel spherical core is 12.3 in. inside diameter with a minimum wall thickness of 0.220 in. Cooling coils of stainless steel tubing, $\frac{1}{4}$ in. outside diameter and 0.028 in. wall thickness, maintain the fuel solution temperature at 80°C during 50 kilowatt operation. A central exposure tube, which accommodates the poison rod used for introducing reactivity, is located along a horizontal diameter. Normal operation of the reactor is controlled with four vertical control rods, which occupy re-entrant thimbles in the core, equally spaced about

the vertical diameter. These rods are normal sintered B₄C and control a total of about 7% reactivity. The reflector consists of reactor-grade graphite bars stacked to form a 56 in. cube. It rests on a concrete pedestal and is completely enclosed with a gas-tight reinforced sheet aluminum container. The core has a volume of 13.6 liters and contains 11.5 liters of enriched uranyl sulphate solution. This fuel loading consisting of 1890 grams of U²³⁵, gives an excess reactivity of 4% at a core temperature of 25°C.

Reactor transients are initiated either by withdrawal of the control rods or by withdrawal of the poison rod from the central exposure tube. The transient neutron level, along with core temperature, core pressure and other pertinent information, is determined with a system of detectors which, with proper amplification, energize light-beam galvanometers in a recording oscillograph. The data records are then produced on photographic paper.

REACTIVITY COEFFICIENTS

It is well known that homogeneous solution reactors have large negative temperature coefficients of reactivity. Free hydrogen and oxygen are also produced in the fuel solution during operation as a result of radiolytic dissociation of the water solvent. The formation of the gas bubbles in the fuel results in an additional negative reactivity coefficient. These two coefficients then form the basis for the self-limiting behavior of the water boiler type reactor. Thus a determination of the values of these coefficients and the dependence of the values on the reactor operating parameters is fundamental to an understanding of the dynamic behavior of the reactor system.

The temperature coefficient of reactivity has been determined over the range from 25°C to 90°C at a core pressure of 68 cm of Hg. The reactivity compensated by core temperature rise was measured over the temperature range indicated. The temperature coefficient of reactivity is then obtained as a function of temperature by taking the first derivative of the experimental curve. The coefficient is $-0.016\% \Delta k / ^\circ\text{C}$ at 25°C and increases in magnitude slowly with increasing temperature to a value of $-0.027\% \Delta k / ^\circ\text{C}$ at

* Atomics International, a division of North American Aviation, Inc., Canoga Park, California.

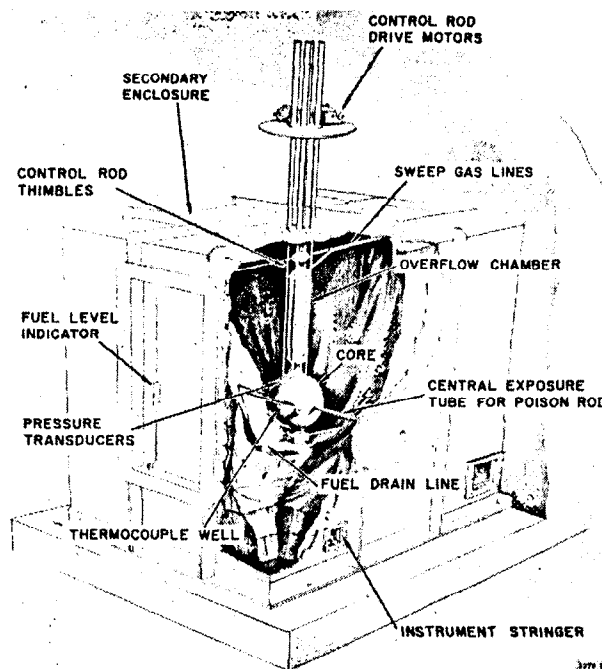


Figure 1. Perspective cutaway of the test reactor installation

about 85°C. Here, as the core temperature approaches the boiling point of the solution, the coefficient increases rapidly and reaches a value of $-0.032\% \Delta k / ^\circ\text{C}$ at 90°C.

The rate of gas production resulting from radiolytic decomposition of water is a function of a number of parameters, including the acidity and uranium concentration of the fuel solution. Only those parameters which influence the transient behavior of the particular reactor under investigation, namely, the pressure, temperature and power, have been investigated.

Measurements of this rate of gas production as a function of the core pressure show the rate to decrease from 15.4 to 13.7 liters/kwh at STP in an essentially linear manner, as the core pressure is increased from 27 to 68 cm Hg at a core temperature of 30°C. Examination of the rate for temperature dependence was conducted over the temperature range from 17 to 90°C at a pressure of about 60 cm of Hg. The results show the rate to be essentially constant at 14.0 liters/kwh at STP, independent of temperature between 30 and 90°C. It decreases slightly to a value of 12.9 liters/kwh at 17.5°C. No significant variation of the rate with reactor power level was detected at powers ranging from 0.5 to 20 kilowatts.

A void coefficient of reactivity has been measured using calibrated volumes in the central exposure tube of the reactor core. Since it is not possible to locate a void inside the welded core assembly the measured results do not necessarily represent a true void coefficient in the reactor. The results show a dependence of the void coefficient on the amount of void volume and gives an asymptotic value of $-0.0026\% \Delta k / \text{cm}^3$. This is to be compared with a void coefficient calculated from temperature effects on re-

activity and the temperature coefficient of expansion of the solution of $-0.0039\% \Delta k / \text{cm}^3$. Determination of reactivity compensation by the voids as a function of position along the central exposure tube shows the coefficient at the center of the sphere to be 1.4 times as large in magnitude as at the edge of the core.

TRANSIENT EXPERIMENTS

The self-limiting behavior of the reactor has been investigated as a function of the significant parameters: amount of reactivity release, rate of reactivity release, initial core pressure and initial core temperature.

With the exception of the studies on the influence of rate of reactivity release, which will be treated separately, all the transients have been initiated with effectively step inputs of reactivity. Other pertinent conditions at initiation of the excursions include the following

1. No cooling water flowing through the core. This will have no real effect on the transient behavior of the system for the shorter reactor periods since the transit time for cooling water flow is about 0.55 second.
2. The reactor gas handling system valved off from the reactor core, so that the radiolytic gases are collected in a ballast system which is evacuated prior to the initiation of the transient.
3. Void volume above the core equal to 2.1 liters.
4. The initial core temperature adjusted to about 25°C, except in the studies on the effects of initial core temperature.
5. Initial core pressure adjusted to one of three values, namely 15.6, 43, and 71 cm Hg.
6. Reactivity inputs varied to give reactor periods ranging from about 80 seconds down to about 4 milliseconds. This corresponds to reactivity releases ranging from about 0.1 to 2.7% Δk .

General Results

As indicated earlier the information on the response of the reactor during the transient power excursions is obtained on recording oscillographs. A reproduction of a typical oscillograph recording is shown in Fig. 2. These data were obtained from an excursion with a reactor period of 6.8 milliseconds and a peak power of 99 megawatts. The reactor power is monitored with two linear channels and two logarithmic channels; however, only one of each is shown in Fig. 2. The output signal from the linear channels is divided and fed to at least two different galvanometers with attenuations which differ by a factor of approximately ten. Thus the more sensitive galvanometers are overdriven, while the less sensitive system gives a complete trace of the power vs. time. The sensitivity of the logarithmic channels is adjusted so that the output saturates prior to the attainment of peak power. The initial sharp increase in the power indicated by the logarithmic channel results from the inherent resistance characteristic of the diode input circuit of the

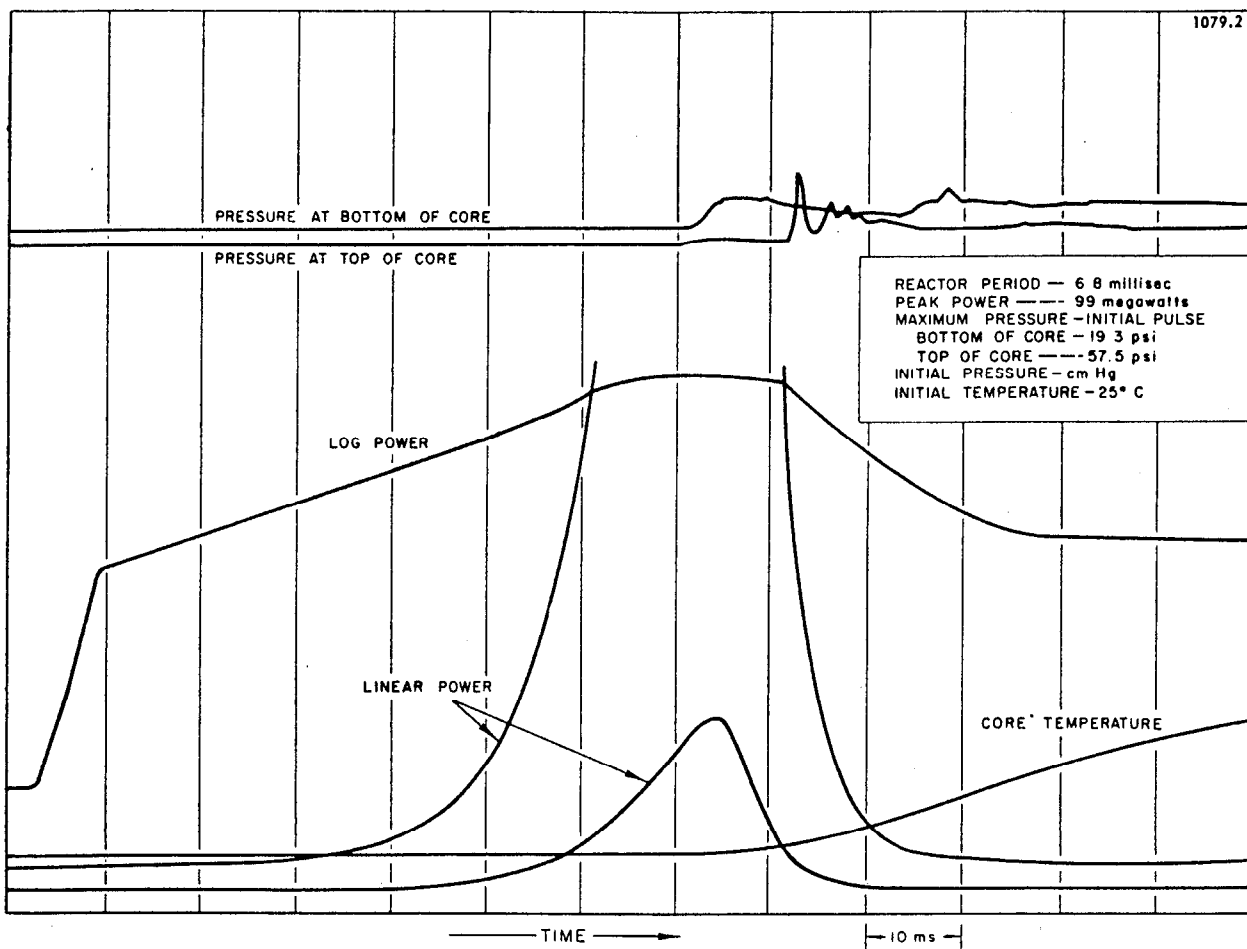


Figure 2. Transient power trace for a reactor period of 4.2 milliseconds

amplifier. This portion of the trace is purely a function of the instrumentation and does not represent the actual power vs. time dependence during the early part of the power excursion. The stable reactor period for the excursion is determined from the two logarithmic power traces and the leading edge of the higher gain linear power traces which indicate the power vs. time history from approximately one to two decades prior to peak power.

The reactor power rises in an exponential fashion until it reaches approximately 10% of the peak value. Intrinsic shutdown of the excursion has begun by this time, so that the rate of power rise deviates markedly from exponential form during the last decade of power increase. After the peak is reached the reactor shutdown is very sharp, so that the power pulse is asymmetric about the power peak. This characteristic asymmetry is noted for reactor periods less than about 0.2 to 0.3 second, and becomes more pronounced with decreasing periods.

The pressure pulse at the bottom of the core is measured with an unbonded strain gauge transducer with the diaphragm in contact with the fuel solution. The initial core pressure is taken as the zero reading for the detector. The pressure rises at a moderate rate to the maximum value of the initial pulse of 19.3 psi. This maximum nearly coincides in this particular

transient with the occurrence of peak power. The pressure gradually diminishes during a period of about 20 milliseconds. It is during this time that fuel is being ejected from the sphere.

The pressure pulse at the top of the core is measured with a similar transducer located about one inch above the normal free surface of the fuel solution. This information channel is also adjusted to give a zero reading at the initial core pressure. It is observed to give a very sharp pressure pulse with a peak of 57.5 psi, with a characteristic smaller second pulse following in about 4 milliseconds. The first pulse, occurring about 10 milliseconds after peak reactor power, is attributed to the striking of the transducer diaphragm by the fuel solution as it is pushed out of the spherical core through the orifice and into the overflow chamber above the critical region.

A summary presentation of the data in the form of peak reactor power as a function of stable reactor period is given in Figs. 3 and 4. This summary includes the data obtained for reactor periods ranging from 80 seconds down to 3.7 milliseconds at values of core pressure equal to 15.6, 43 and 71 cm Hg.

In general, the transients initiated at lower core pressures are observed to yield lower peak powers. For reactivity inputs up to about 0.8% Δk , corresponding to the "prompt critical region", increasing the pressure

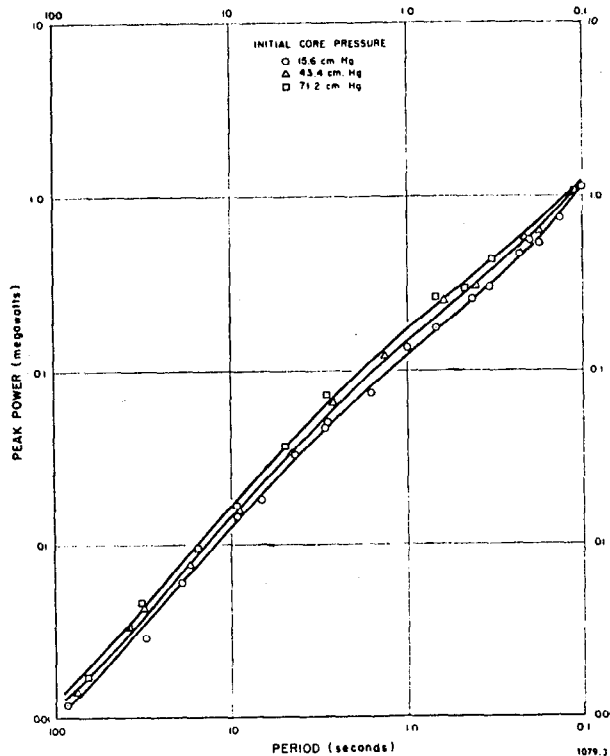


Figure 3. Peak reactor power vs. reactor period for periods ranging from 80 seconds to 100 milliseconds

from 15.6 to 71 cm Hg results in an increase of about 20% in the peak power. This pressure effect appears to diminish in the prompt critical region; that is for, reactor periods of about 0.3 down to 0.07 second. At the lower periods it then becomes more pronounced, so that an increase of the initial pressure from 15.6 to 71 cm Hg results in an increase in peak power of about 50%. Except for the reduced effect in the prompt critical region, a pressure dependence of the type observed is to be expected qualitatively, because of the increased reactivity compensation by the radiolytic gas produced at the much lower pressure. However, a quantitative description and understanding is not yet available and requires further study and information on the formation of the radiolytic gas bubbles.

The power traces have been integrated to obtain the energy release in the transient power burst. Results for excursions initiated at a core pressure of 15.6 cm Hg are shown in Fig. 5 which presents energy release as a function of reactor period. These results do not cover the range of lower reactivity releases. For reactor periods below about 0.3 to 0.4 second the energy release in the power burst is not defined unambiguously.

Transient Pressures in the Core

The transient pressures inside the core are observed to be initiated with reactor periods of about 30 milliseconds. These pressures are the result of the formation of radiolytic gas in the fuel solution with the subsequent displacement and eventual expulsion of

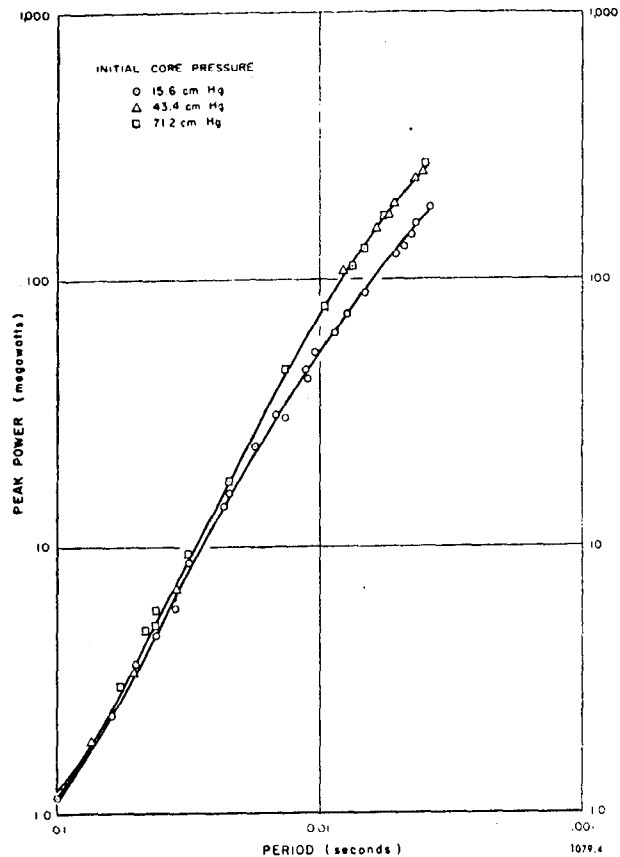


Figure 4. Peak reactor power vs. reactor period for periods ranging from 100 to 3.7 milliseconds

the solution from the core. Not only can they seriously affect the dynamic behavior of the reactor,³ but knowledge of the peak values is required for proper engineering design of reactor vessels. The variation of the transient pressure pulses at both the top and bottom of the core with reactor period is shown in Fig. 6. The pressure pulse at the bottom of the core increases with decreasing reactor period to a maximum of about 40 psi at a period of 4 milliseconds.

At the top of the sphere the pressure pulse, which appears with reactor periods of about 20 milliseconds, first occurs as expulsion of the fuel solution from the core is observed. This pulse also increases with decreasing reactor period, but reaches a higher value of about 100 psi at periods of 4 milliseconds. In all experiments performed the pressure developed at the top of sphere is the largest pressure observed.

Temperature Dependence

Examination of the dependence of the transient behavior of the reactor on initial core temperature has been conducted with reactivity inputs of 0.4 and 0.7% Δk to give reactor periods of 6.6. and 0.63 second respectively. An initial core pressure of 15.6 cm Hg was chosen for this investigation, since it was desired conveniently to approach the boiling point of the fuel solution with the temperatures at which the excursions were initiated. This pressure results in a fuel solution boiling point of about 61°C. The initial core tempera-

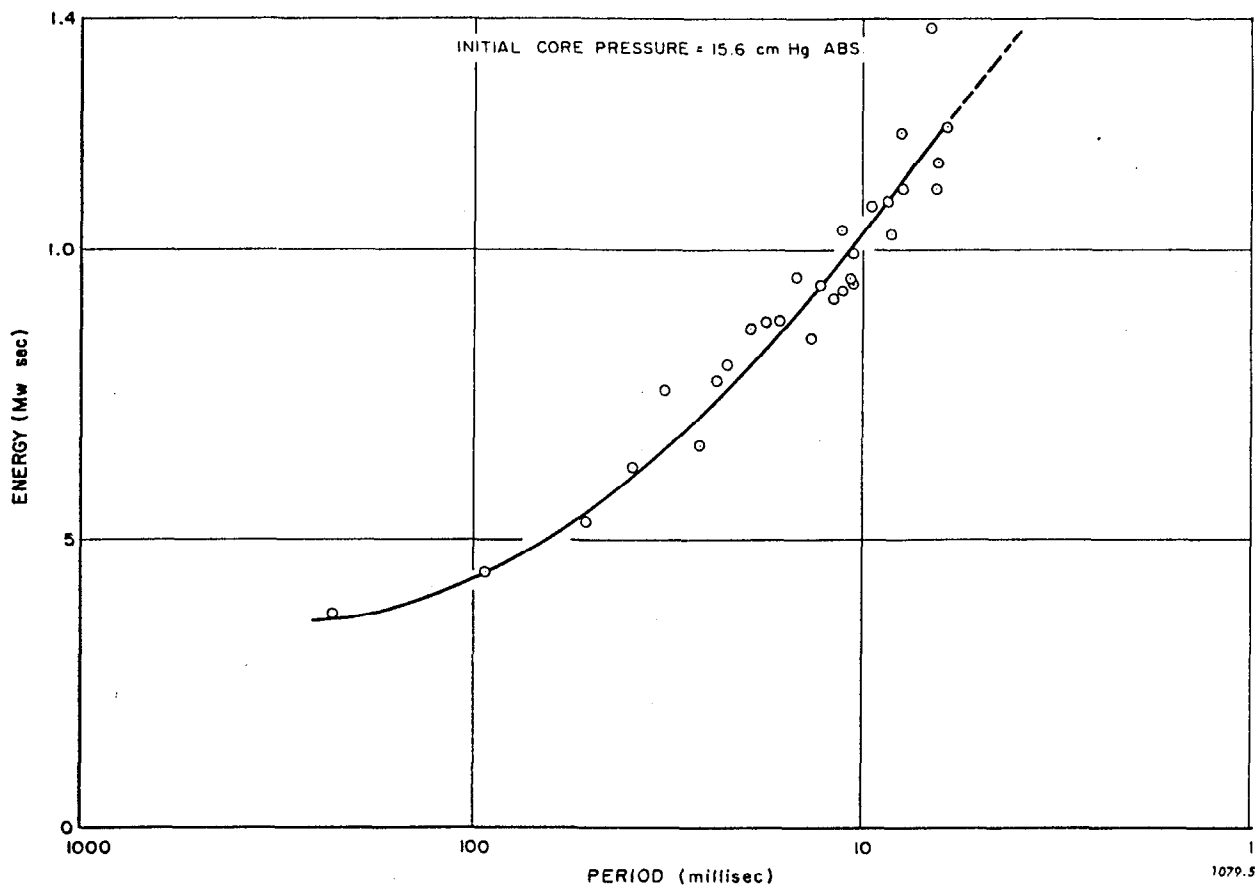


Figure 5. Total energy release in power excursion as a function of reactor period for initial core pressure of 15.6 cm Hg

ture was varied from 16 to 61°C for the 0.4% releases and from 25 to 45°C for the 0.7% releases.

Results from this investigation are shown in Fig. 7, in which peak reactor power is plotted as a function of the initial core temperature. In each case the peak power is observed to decrease in an essentially linear fashion with increasing temperature at the lower temperatures. This decrease is attributed to the increased water vapor content of the gas bubbles in the core as a result of the increase in the partial pressure of the vapor with rising core temperature.

Above about 50°C there is a rapid decrease in the peak power from the smaller reactivity release. This is interpreted to result from localized boiling in the core during the excursion. Boiling of the solution is confirmed by the detection of violent bubbling in the core through sound monitoring during these transients initiated at the higher temperature. The marked decrease in peak power as the initial temperature reaches the boiling point shows the pronounced effect of boiling as an additional shutdown mechanism in the homogeneous solution reactor.

For the larger reactivity release of 0.7% Δk , which results in much higher peak powers, the sharp decrease in peak power begins to occur at about 40°C. Thus initiation of boiling occurs with a much lower initial core temperature because of the larger energy

densities which occur during these transients. Consequently, the boiling makes a much greater relative contribution to the reactor shutdown.

Ramp Reactivity Inputs

Reactivity inputs which increase linearly with time are representative of typical accidents which can occur with operating reactors. Accordingly, power excursions have been initiated by inserting reactivity with ramp rates of 0.032, 0.063, 0.095 and 0.126% Δk /second. The insertions were initiated with the reactor at essentially zero power and with the core temperature at 25°C with no coolant flow. The ramp releases were terminated with two values of total reactivity input, namely, 1.2 and 2.4% Δk . Minimum observed reactor periods ranged from 0.46 second for the slowest ramp to 0.062 second for the maximum ramp. The excursions were allowed to continue for a period of 1.5 minutes after reaching peak power. At this time the reactor was shut down manually.

A typical sequence during a ramp input is a rapid rise in reactor power, resulting in a relatively sharp power pulse, followed by a minimum and then a slow increase in power during the remainder of the interval in which the reactivity is being inserted. Highly damped oscillations of small amplitude with periods between 2 and 3 seconds may occur during this

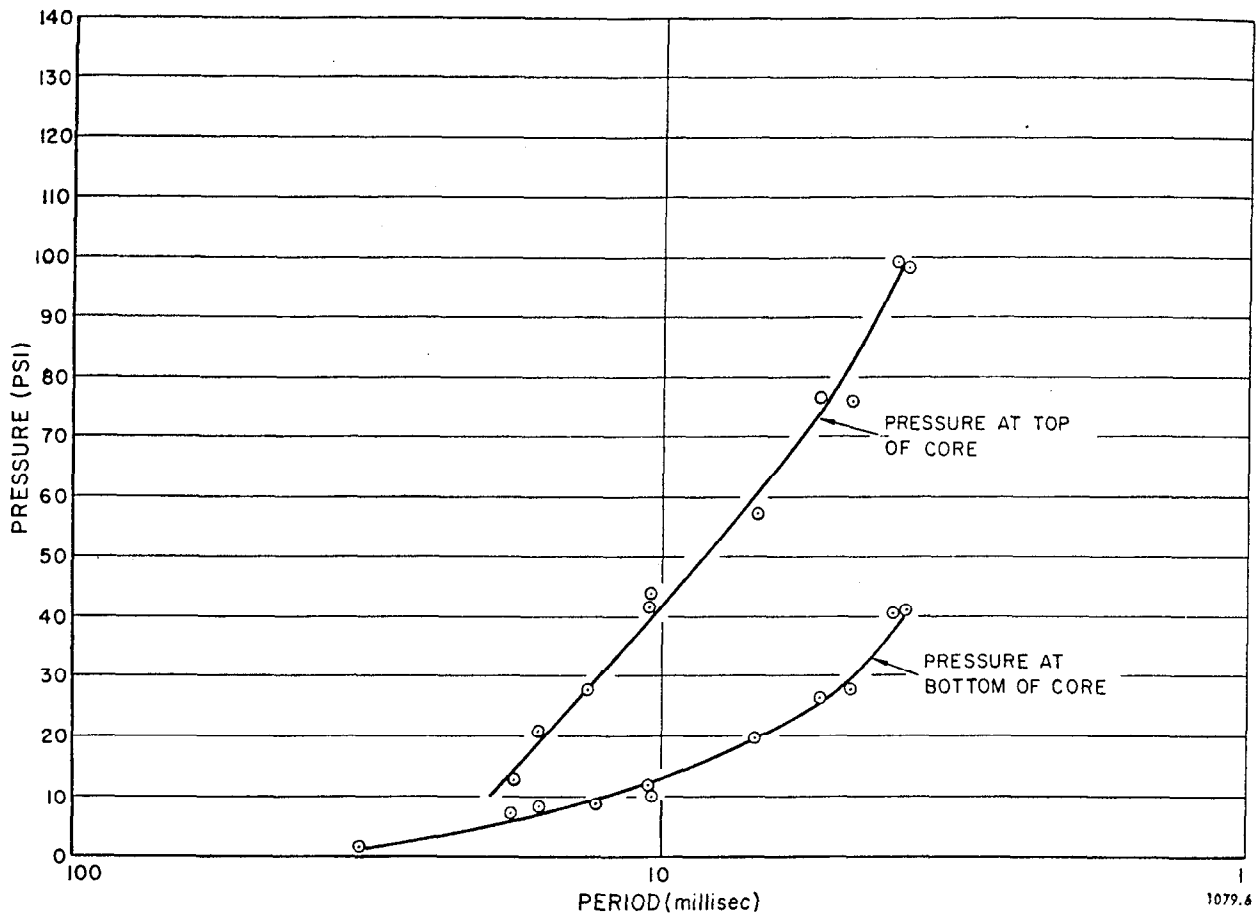


Figure 6. Peak transient pressures in reactor core as functions of reactor period

interval. After the ramp is stopped, the power level approaches an equilibrium value determined by the static coefficients of reactivity and the total input from the ramp. No unstable behavior was observed during any phase of the transients.

A summary of the results showing peak reactor power as a function of ramp rate is given in Fig. 8. Within the range of reactivity insertion rate investigated, the peak power is independent of the total reactivity input, since the peak is attained considerably before total input is achieved. Rather the power peaks are found to correspond to those obtained from step input transients with reactor periods similar to the minimum periods observed during the ramp studies. Thus with this range of reactivity input rates, sufficient energy release and resultant reactivity compensation occurs early enough in the power history of the excursion to eliminate the dependence on the total amount of reactivity released. The total reactivity input manifests itself only in the equilibrium power reached after the initial power burst. Average power levels of 25 and 40 kilowatts respectively were found for the two values of total reactivity input, 1.2 and 2.4% Δk .

These equilibrium power levels are, of course, dependent on other parameters such as the initial core temperature, core pressure and rate of coolant flow.

This is illustrated by the ramps of 0.126% Δk /second, initiated with full coolant flow of 15 gpm. Under this condition no effect on the peak power during the transient pulse was observed (see Fig. 8), but the equilibrium power after the transient pulse was 160 kilowatts.

ANALYSIS

The analytical work has been directed along two major lines: 1, computation of the time-dependent reactivity from the experimentally determined power history of an excursion, to be used in development of a model for the reactor shutdown mechanisms; and 2, application of the model in analytic predictions of the reactor behavior leading to the continued improvement and extension of the model.

Figure 9 shows the experimentally determined power history resulting from a reactor period of 32 milliseconds, together with the energy and reactivity curves computed from it. The initial pressure was 15.6 cm Hg. Note the extreme sweep of reactivity to large negative values, as might be expected from the relatively sharp drop in power immediately after the peak. Reactivity determined in this way will, however, be subject to errors arising from the failure of the kinetic equations in the case of large departure from $k_{eff}=1$.

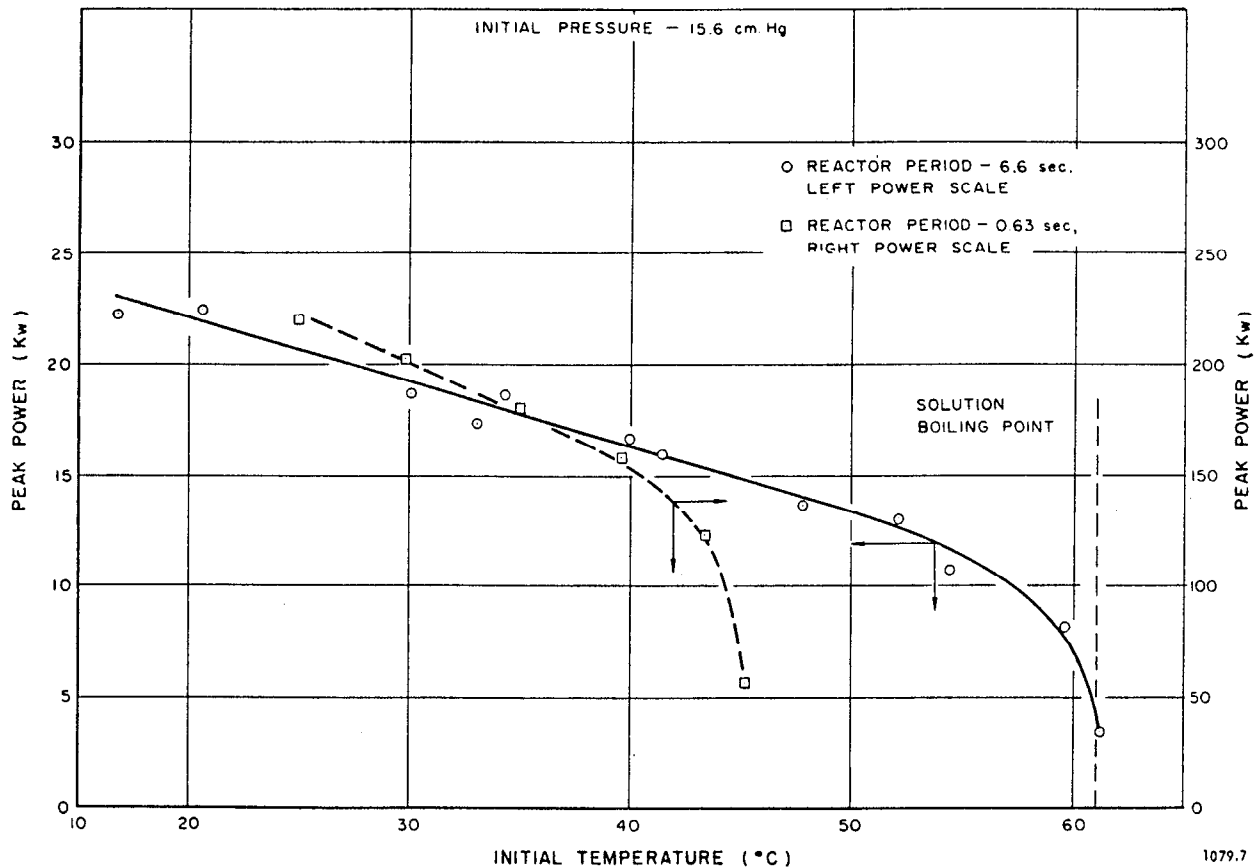


Figure 7. Variation of peak reactor power with initial core temperature for reactivity releases of 0.4 and 0.7% Δk

Figure 10 shows a similar computation for a reactor period of 12 milliseconds initiated at the same initial pressure.

Note that the shut-down is relatively more rapid for the shorter period, in agreement with the general observation that the ratio of the energy released after the instant of peak power to the total energy in the burst is found to decrease with decreasing reactor period.

An important result of these and similar computations in this range is that the energy produced up to the time of peak power is consistently more than ten times the amount needed to reduce the reactivity to one dollar, provided one makes the apparently unjustified assumption that radiolytic gas bubbles are produced instantaneously. At the same time the reactivity compensation at peak power, computed solely from the observed energy production, the heat capacity and the temperature coefficient of reactivity, is consistently a minor fraction of the total compensation. It is concluded, therefore, that gas production is dominant as a shutdown mechanism for periods in the range from approximately one second to four milliseconds.

The most recent model to be applied to the analytic predictions of the reactor behavior is described by the following set of equations:

Neutrons:

$$\frac{dN}{dt} = \frac{\beta}{\ell} \left[(R-1)N + \sum_{i=1}^6 f_i W_i \right], \quad (1)$$

$$\frac{dW_i}{dt} = \lambda_i(N - W_i), \quad i=1, \dots, 6.$$

Temperature:

$$\frac{dT}{dt} = K(N - N_0) - \gamma T. \quad (2)$$

Dissolved radiolytic gas:

$$\frac{dB}{dt} = G(N - N_0) - \nu B. \quad (3)$$

Void volume:

$$\frac{dV}{dt} = \nu B - \sigma V. \quad (4)$$

Reactivity:

$$R = R_0(t) + aT + \phi V. \quad (5)$$

The symbols which need further definition are:

R = reactivity in dollars

f_i = relative yield of the i th delayed neutron precursor

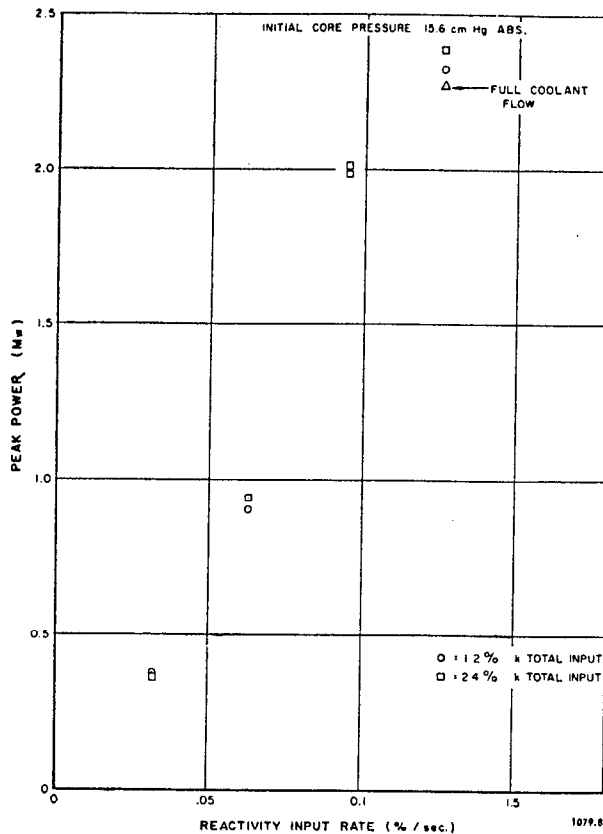


Figure 8. Peak reactor power vs. reactivity input rate

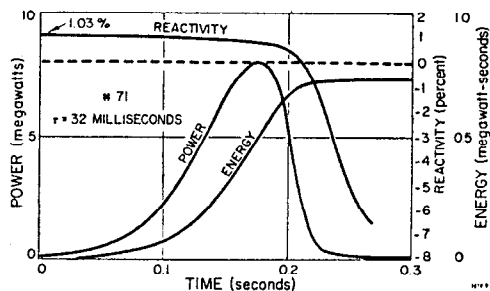


Figure 9. Power, energy and reactivity during a transient with a reactor period of 32 milliseconds in KEWB

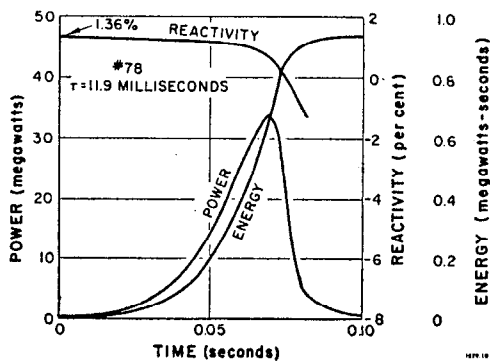


Figure 10. Power, energy and reactivity during a transient with a reactor period of 12 milliseconds in KEWB

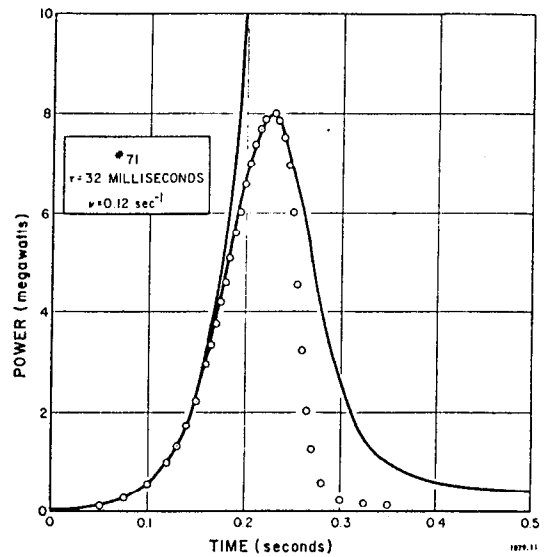


Figure 11. Experimental power trace compared with theoretical calculation for reactor period of 32 milliseconds

- W_i = relative concentration of the i th delayed neutron precursor
- λ_i = decay constant for the i th delayed neutron precursor
- K = reciprocal heat capacity
- γ = reciprocal of heat transfer characteristic time (negligible)
- G = rate of radiolytic decomposition of water
- ν = reciprocal of bubble formation delay time
- σ = reciprocal of bubble residence time (bubble escape time)
- R_0 = input reactivity
- α = temperature coefficient of reactivity
- ϕ = void volume coefficient of reactivity.

The set of Eqs. (1) is also that used to compute the reactivity from the experimental power traces by solving for reactivity and using a numerical integration process to determine the W_i 's. The variables T , B and V are taken to be departures from some suitable equilibrium value, so that B might be interpreted as a measure of the supersaturation at any time.

Parameters used in the computations reported here are as follows:

- $\beta/l = 128 \text{ sec}^{-1}$
- $l = 62.5 \text{ microseconds, if } \beta = 0.008$
- $\alpha = -0.02 \text{ dollars}/^\circ\text{C}$
- $K = 0.02 \text{ }^\circ\text{C}/\text{kw-sec}$
- $\gamma = 0.01 \text{ sec}^{-1}$
- $\phi = -0.005 \text{ dollars}/\text{cm}^3$
- $G = 4 \text{ cm}^3/\text{kw-sec at S.T.P.}$
- $\sigma = 1 \text{ sec}^{-1}$
- $\nu = \text{adjustable parameter.}$

Relative yields and decay constants for the delayed neutrons are the measured values reported from Los Alamos Scientific Laboratory⁴ for thermal fission of U^{235} . The value of β/l is determined independently from pile oscillator phase shift measurements and from control rod displacements in fast excursions; thus far, data from the former method are perhaps valid to

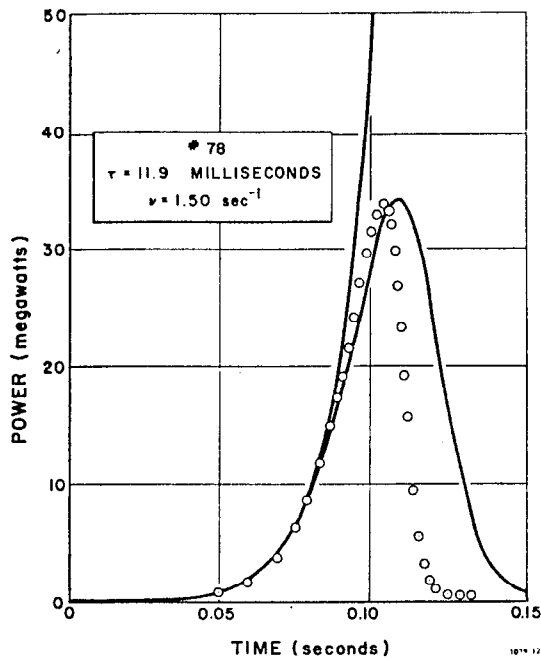


Figure 12. Experimental power trace compared with theoretical calculation for reactor period of 12 milliseconds

within $\pm 30\%$, while the latter method has a limit of error of approximately $\pm 10\%$.

The temperature coefficient of reactivity is that measured statically at 25°C , rounded off to one significant figure. The heat capacity is that for the 11.5 liters of fuel solution only. The time scale for heat transfer is estimated from the known contribution of thermal expansion to the reactivity input required to maintain steady operation in the kilowatt range.

The void coefficient of reactivity is that calculated from the temperature coefficient of reactivity and the thermal expansion coefficient of the solution. The gas production rate is that determined statically for a wide range of temperature, pressure and reactor power level.

Both the bubble formation delay time and the bubble residence time have been considered as adjustable parameters. However, for the set of experiments under discussion, the value of σ has very little effect on the computed peak power once all the other parameters except ν are fixed. Hence, an estimated value of $\sigma = 1 \text{ sec}^{-1}$ was selected for the computations reported here.

Figures 11 and 12 show the comparison of analogue computations of reactor power (the solid curve which has a peak) with points taken from the experimental power traces. In these two figures, the solid line which rises monotonically is an exponential having the same period as the actual reactor power.

In these computations, the single parameter ν was adjusted until the experimental peak power was matched. The values of ν shown in the figures, which correspond to bubble delay times of 8 seconds and two-thirds of a second, were obtained in conjunction with the assumption that $G = 4 \text{ cm}^3/\text{kw-sec}$. Inasmuch as these excursions were started with a system pressure

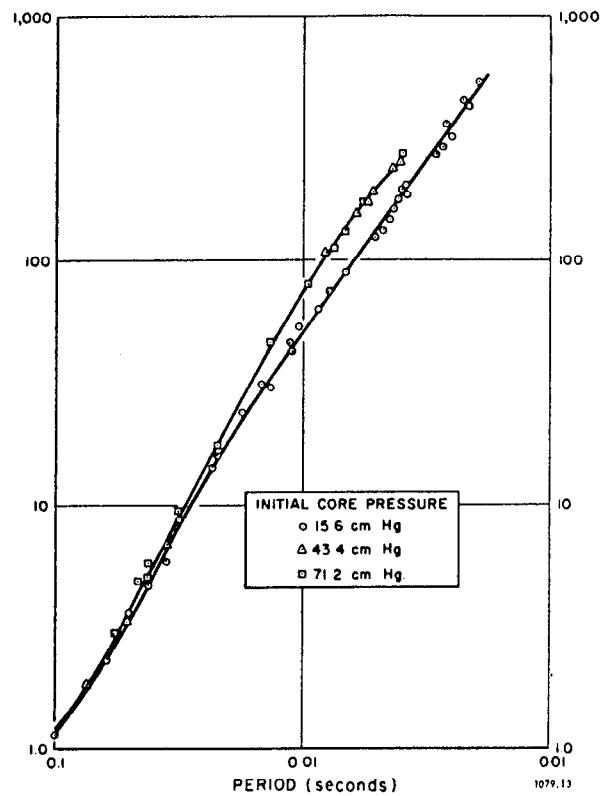


Figure 13. Peak reactor power vs. reactor period for periods ranging from 100 to 2.0 milliseconds

of 15 cm Hg, a more appropriate value of $G = 20 \text{ cm}^3/\text{kw-sec}$ was used first, with resultant values for the bubble delay time required to match peak power which seemed extremely large (40 seconds and 3 seconds for the corresponding cases). However, the shapes of the computed curves were not altered by this change in the value of G and the compensating change in ν required to maintain the peak power.

The experimental curves are more sharply peaked in relation to the computed curves, especially for shorter periods, indicating the need for further improvements in the simulator model. The most promising approach to the problem of analytically reproducing the pulse shape appears to be the inclusion of non-linear terms for radiolytic gas formation, and the addition of a model for the dependence of the effective gas-produced void on instantaneous bubble pressures.

The analytical efforts to date have resulted in a model which gives an approximate description of the dynamic behavior of the reactor. However, improvements are needed for a more accurate description and better analytic predictions of the transient characteristics. These improvements are continually being added to the theory, and much success is expected as more experimental data are collected and the theoretical studies continue.

The experiments have provided a dramatic demonstration of the inherent safety of the homogeneous solution type reactor. Transient power excursions have been initiated to give reactor periods shorter than

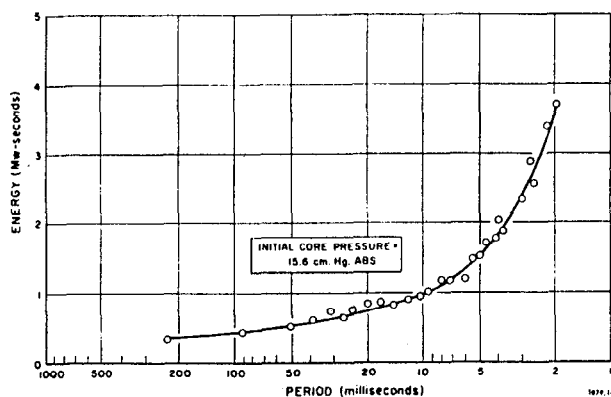


Figure 14. Energy release in first burst as a function of reactor period

those observed in any other type of thermal reactor except where extensive damage resulted.⁵ These excursions have been shown to be completely controlled by the self-limiting characteristics of the reactor with the generation of only moderate pressures in the core.

SUPPLEMENT

This supplemental information is concerned only with reactor transients involving periods between 3.7 and 2.0 milliseconds with the reactor system at an initial pressure of 15.6 cm of Hg.

Peak Power as a Function of Reactor Period

Step reactivity inputs have been systematically increased to the planned limit of a 0.002 second period. The maximum power observed in the 0.002 second period test was 530 megawatts. Peak power as a function of reactor period is graphically represented in Fig. 13.

Energy Release as a Function of Reactor Period

Figure 14 presents the energy releases in the first burst for the transients conducted down to the 2.0 millisecond period. The maximum energy release is slightly less than 4.0 megawatt-seconds, equivalent to about 1½ minutes of normal operation of this type reactor.

Peak Pressures as Functions of Reactor Period

The characteristic second pressure pulse, which was observed at the top of the core during power transients involving periods down to 3.7 milliseconds, became the

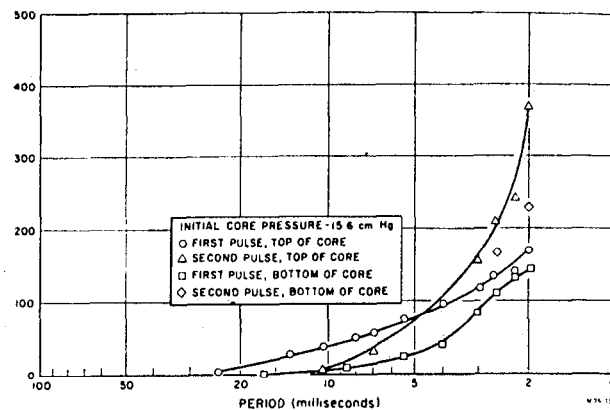


Figure 15. Transient pressures in reactor core as functions of reactor period

highest indicated pressure in those transients having periods between 3.7 and 2.0 milliseconds. A similar second pulse developed at the bottom of the reactor core in the faster transients. This pressure wave became larger in magnitude than the initial pulse detected at that location during a given excursion. These second pulses were generally observed to be much more sharply defined than the initial pulse generated at the bottom of the core, which is shown in Fig. 2. The maximum pressure observed in the course of the fastest transient was 370 psi, which was detected at the top of the sphere. The pressure data are summarized in Fig. 15.

ACKNOWLEDGEMENTS

This paper represents the results of a four-year effort. During this time many people, other than the authors, have contributed to the program. These people, with their contributions, are gratefully acknowledged below:

Grant Schumann (July 1955), reactor installation operation and testing. Eugene B. Hecker (September 1955), instrumentation installation and reactor testing. John B. Williams (October 1954–June 1956) design of facility and reactor components. Leo P. Inglis (October 1954–May 1956), design of instrumentation and control systems. Gerl C. Murphy (January 1957), data reduction. Bernard R. Moskowitz (October 1955–October 1956), reactor installation and initial testing. John C. Moore (September 1957), instrumentation for reactor tests. Robert C. Allen (July 1956–November 1956), instrumentation installation and testing.

REFERENCES

1. P. R. Kasten, *Reactor Dynamics of the Los Alamos Water Boiler*, Nuclear Eng., Part I, American Institute of Chemical Engineers, 229 (1954).
2. J. W. Flora, J. W. Shortall and W. E. Drummond, *Temperature Effect on Reactivity of the C.R. and D. Water Boiler*, LRR-148 (1954).
3. M. E. Remley, J. W. Flora, D. L. Hetrick and L. P. Inglis, *Program Review of the Water Boiler Reactor Kinetic Experiments*, NAA-SR-1525 (1956).
4. G. R. Keepin, T. F. Wimett and R. K. Ziegler, *Delayed Neutrons from Fissionable Isotopes of Uranium Plutonium, and Thorium*, Phys. Rev., 107, 1044 (1957).
5. J. R. Dietrich, *Experimental Determinations of the Self-Regulation and Safety of Operating Water-Moderated Reactors*, Proceedings of the International Conference on the Peaceful Uses of Atomic Energy, Geneva 1955, P/481, Vol. 13, p. 88, United Nations, New York (1956).